JOURNAL OF SPACECRAFT AND ROCKETS
Vol. 48, No. 3, May–June 2011

Electric Propulsion System Selection Process for Interplanetary Missions

Damon Landau,* James Chase,† Thomas Randolph,‡ Paul Timmerman,§ and David Oh¶
Jet Propulsion Laboratory, California Institute of Technology, Pasadena, California 91109-8099

DOI: 10.2514/1.51424

The disparate design problems of selecting an electric propulsion system, launch vehicle, and flight time all have significant impacts on the cost and robustness of a mission. The effects of these system choices combine into a single optimization of the total mission cost, where the design constraint is a required spacecraft net (nonelectric propulsion) mass. Cost-optimal systems are designed for a range of mass margins to examine how the optimal design varies with mass growth. The resulting cost-optimal designs are compared with results generated via mass optimization methods. Additional optimizations with continuous system parameters address the impact on mission cost due to discrete sets of launch vehicle, power, and specific impulse. The examined mission set comprises a near-Earth asteroid sample return, a multiple main belt asteroid rendezvous, a comet rendezvous, a comet sample return, and a mission to Saturn.

Nomenclature

C_3	=	launch energy parameter (V_∞^2), km^2/s^2
I_{sp}	=	specific impulse, s
$\dot{m}$	=	thruster mass flow rate, kg/s
m_{C3}	=	launch mass at interplanetary injection ($C_3 \geq 0$), kg
m_f	=	delivered mass to final target, kg
m_N	=	non-solar-electric-propulsion net mass, kg
m_p	=	propellant mass, kg
m_0	=	mass at Earth escape (C_3 of zero), kg
P_0	=	solar array power at 1 astronomical unit
T	=	thrust, N
V_∞	=	hyperbolic excess velocity, km/s
ΔV	=	change in velocity, km/s
μ_{P0}	=	power mass coefficient, kg/kW
μ_p	=	propellant mass coefficient, kg/kg
χ_{m0}	=	launch vehicle cost coefficient, $/kg
χ_{P0}	=	power cost coefficient, $/kW
χ_p	=	propellant cost coefficient, $/kg
χ_{TOF}	=	flight-time cost coefficient, $/year

I. Introduction

RECENT missions such as Dawn [1], SMART-1 (Small Missions for Advanced Research in Technology-1) [2], and Hayabusa [3] demonstrate the expanding role of solar electric propulsion (SEP) in the robotic exploration of our solar system. As future missions with electric propulsion are planned, traditional design techniques, largely developed for chemical propulsion systems, may prove inadequate. For example, with chemical propulsion, the spacecraft trajectory can mostly be designed independently of the launch vehicle, which is selected to accommodate the spacecraft mass; power and the propulsion system design have a secondary effect on the available mass. With electric propulsion missions, the launch vehicle, solar array power, and number and type of thrusters combine to affect the spacecraft trajectory and delivered mass, requiring concurrent design of these systems [4–6]. The flight time to the target also alters the trajectory and may affect the feasibility of a mission. We therefore explore how variations in these four key parameters (launch vehicle, power level, thrusters, and flight time) affect the design of an interplanetary mission. Moreover, the discrete levels of available systems can cause suboptimal performance (e.g., the actual engine thrust may be lower than desired, thus increasing trajectory ΔV). The effect of discrete hardware choices on SEP system design is also addressed. Results are provided for an assumed mission set comprising a near-Earth asteroid sample return, a main belt asteroid rendezvous (e.g., Dawn), a comet rendezvous, a comet sample return, and a mission to Saturn.

Key issues to be resolved during preliminary design include selecting a launch vehicle, solar array size, thruster type, and flight time. Usually, the mission target (or short list of potential targets) and spacecraft net mass are chosen to satisfy scientific objectives. Net mass is defined as any mass that is unaffected by variations in the SEP system: i.e., mass of the payload, spacecraft bus, hydrazine, supporting structure, etc. Therefore, the net mass allocation is treated more as a constraint than as a free design parameter. (Initial iterations between mission designers and science investigators ensure that the desired net mass range and destination set are feasible for the given time frame and budget of the mission.) The problem then becomes selecting a spacecraft system, defined by the four aforementioned parameters, that is cost effective and provides the required net mass while being robust to fluctuations in the design. A straightforward solution is to minimize mission cost for a given net mass. (The term "cost" always refers to the dollar cost of the mission.) This approach handles the cost-effective requirement while examining optimal cost solutions over a range of net masses, addressing the robust requirement. The resulting trajectories are better suited to a given mission than those generated via traditional mass optimization, because mission optimization more directly influences the trajectory design process. By further ensuring that the spacecraft system produces viable trajectories over a range of neutral mass, the resulting missions are better suited to a given trajectory than those produced via point design methods, because the full span of optimal trajectories influences the mission design process. This coupling of mission and trajectory optimizations produces a cost-efficient design that is able to absorb variations in net mass and SEP system performance.

Presented as Paper 2008-7362 at the AIAA/AAS Astrodynamics Specialist Conference, Honolulu, HI, 18–21 August 2008; received 1 July 2010; revision received 22 December 2010; accepted for publication 22 December 2010.

*Engineer, Trajectory Design and Navigation, Mail Stop 301-121. Member AIAA.
†Staff Engineer, Flight Systems Engineering, Mail Stop 264-623. Member AIAA.
‡Project Element Manager, Propulsion and Materials Engineering, Mail Stop 125-109. Senior Member AIAA.
§Senior Power Systems Engineer, Power Systems, Mail Stop 303-310K.
¶Senior Engineer, Flight Systems Engineering, Mail Stop T1722. Senior Member AIAA.

II. Trajectory and System Models

A. Trajectory Model

The trajectories are optimized using the Jet Propulsion Laboratory Mission Analysis Low-Thrust Optimizer (MALTO) [7]. The key aspect of MALTO is that it approximates continuous thrusting by a series of impulsive thrust vectors connected by conic arcs, as illustrated in Fig. 1, which contains a cartoon of a simplified problem to illustrate the model. The magnitude of thrust on each segment is bounded by the power available, the engine model, and the segment duration. During the optimization, MALTO propagates a trajectory forward and backward from control points (e.g., planets), and continuity is enforced by constraining the spacecraft states to be equal at the match points.

The underlying optimizer in MALTO is SNOPT [8], which is based on a sequential quadratic programming algorithm. Three different objective functions and constraint sets are used for the trajectory analysis:

1) Maximize delivered mass with constrained time of flight (TOF), P_0, I_{sp}, and launch vehicle m_0 with free m_p.

2) Maximize net mass with constrained TOF, I_{sp}, and launch vehicle m_0 with free P_0 and m_p (for given μ_{P0} and μ_p).

3) Minimize flight time with constrained delivered mass, P_0, I_{sp}, launch vehicle m_0, and m_p. This last mode is applied once the hardware and spacecraft mass values have converged. Longer flight times generally deliver more mass but cost more for extended operation time. While the exact cost depends on the mission, a TOF cost factor of $\chi_{TOF} = \$10$ million/year is used to balance the benefit of additional mass against cost of operations.

B. Optimization of Cost and Net Mass

MALTO does not explicitly optimize trajectories for minimum cost (i.e., χ_{TOF}, χ_{P0}, χ_{m0}, and χ_p are not optimization parameters), so mission dollar cost is minimized by a two-step process of a grid search (to explore the broad design space) and a simplex search (to refine the optimal solution) on TOF, P_0, and I_{sp}. (The inclusion of the cost parameters would make the process much simpler, but there are currently no plans for MALTO's programmers to alter the program in this way.) It is also not possible to constrain net mass in MALTO, so m_0, P_0, m_p, and m_f are simply scaled to provide a desired net mass. This scaling operation is possible because different spacecraft with the same acceleration history will travel along the same trajectory (with the same optimal launch date, C_3, ΔV, etc.). The launch vehicle model is designed so that the launch mass at a given C_3 (m_{C3}) is proportional to m_0 (mass at escape, $C_3 = 0$), and the thrusters are modeled with constant I_{sp} (so thrust T and mass flow $\dot{m}$ are proportional to P_0), which causes the thrust-to-mass ratio (acceleration) to be consistent. (More accurate launch vehicle and thruster performance curves replace these idealized models once a preliminary design is chosen.) This scaling property is particularly useful for examining a range of net masses. For example, if a mission with specified m_0, TOF, P_0, and I_{sp} optimizes to launch mass $= m_{C3}$, delivered mass $= m_f$, and propellant mass $= m_p$, then the net mass is given by Eq. (1):

$$m_N = m_f - \mu_{P0}P_0 - \mu_p m_p \tag{1}$$

Then, if m_N^* is the desired net mass, the design parameters are adjusted by Eqs. (2) and (3):

$$f = m_N^*/m_N \tag{2}$$

$$m_0^* = fm_0, \qquad P_0^* = fP_0, \qquad m_f^* = fm_f, \qquad m_p^* = fm_p \tag{3}$$

The acceleration history is the same, because the launch vehicle and thruster models are designed to satisfy Eq. (4):

$$m_{C3}^* = fm_{C3}, \qquad T^* = fT, \qquad \dot{m}^* = f\dot{m} \tag{4}$$

Thus, a spacecraft with any desired net mass follows the same trajectory as the original spacecraft design. In this formulation, m_0, TOF, P_0, and I_{sp} are independent design parameters and m_f, m_p, m_{C3}, T, and $\dot{m}$ are derived parameters from the optimal trajectory. The mission cost (or at least the aspects of cost affected by the trajectory design) is then minimized by varying TOF, P_0, and I_{sp}. The objective function is the relative cost, which accounts for variations from an arbitrary baseline:

$$\text{relative cost} = \chi_{m0}m_0^* + \chi_{P0}P_0^* + \chi_p m_p^* + \chi_{TOF}\text{TOF} \tag{5}$$

The terms in Eq. (1) do not account for the total mass of a system. For example, the power system term $\mu_{P0}P_0$ only accounts for variations in mass, as the fixed mass does not affect the optimization. Instead, any fixed masses are lumped with the net mass, which is defined as the mass that is unaffected by changes in the SEP system. So if the power system model is 100 kg + 10 kg/kW, the 100 kg is added to the net mass and μ_{P0} is 10 kg/kW (and not the total specific mass of the system). Similarly, from Eq. (5), it is evident that the outcome of this approach is not to minimize the comprehensive cost of the mission, as there is no accounting for instrument or spacecraft bus costs. Moreover, this expression does not even account for the total cost that is affected by mission design choices. Instead, it provides the difference in cost from a baseline due to varying any of the key mission design parameters so that a stationary point may be found where any variation in flight time, power, or specific impulse results in an increase in cost for a given net mass. Thus, just as a set of mass coefficients are readily applicable to maximize mass fractions [9,10], an extended parameter set that includes cost coefficients may be applied to the cost-optimization problem.

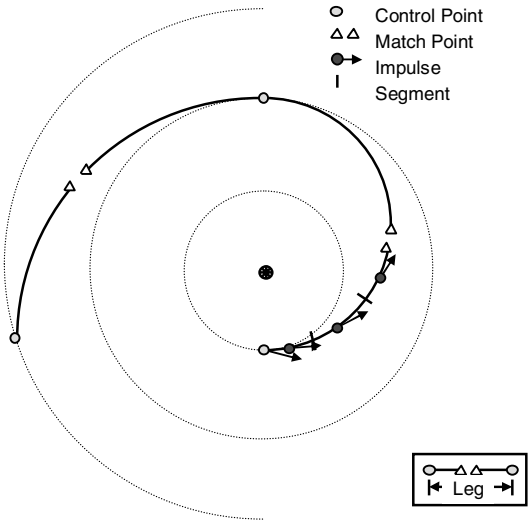

Fig. 1 Schematic of MALTO trajectory model [7].

C. Launch Vehicle

The launch vehicle model is designed to approximate the performance of existing launch vehicles while allowing the launch mass to scale proportionally with m_0. As demonstrated in Fig. 2, the chosen polynomial in C_3 (determined heuristically) fits a range of launch vehicles and allows free choice of launch mass by selecting m_0 for a given C_3 (which is optimized in MALTO). The launch vehicle curves are published by Kennedy Space Center.**

While much insight is gained by examining the mission design problem with free choice of launch vehicle size, there are only a handful of launch vehicles that fit a specific mission. Therefore, the design problem is also addressed with a launch vehicle set limited to $m_0 = 1.5, 3.5, 5, 6.5$, and 9 t. These values very roughly (within half a ton) correspond, respectively, to the Delta II Heavy, Atlas 401, Atlas 531, Atlas 551, and Delta IV Heavy launch vehicles. The launch vehicle cost factor χ_{m0} is assumed to be \$20 million/t. It is emphasized that this value is not used to determine the absolute cost

**Data available at http://elvperf.ksc.nasa.gov [retrieved 1 August 2008].

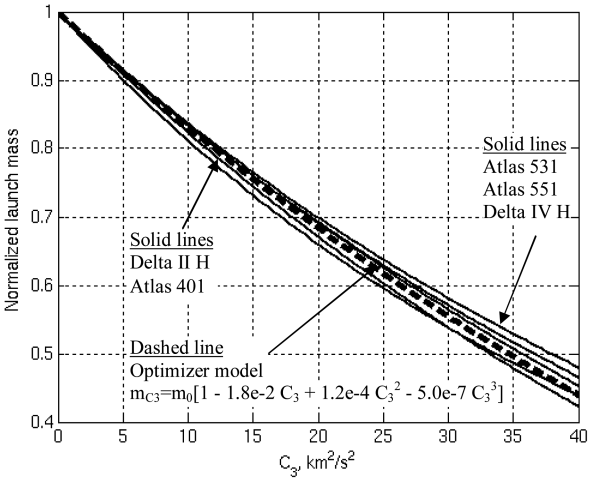

Fig. 2 Launch vehicle model approximates actual performance.

of a launch vehicle but, rather, to estimate the relative costs of switching between launch vehicles.

D. Thrusters and Propellant

The thrusters are modeled as an ideal engine, meaning that the thruster operates at any input power, and the efficiency η and specific impulse I_{sp} are assumed to be constant. These assumptions result in a thrust T and mass flow rate $\dot{m}$ that are determined by Eq. (6), where the efficiency is assumed to be 60% [11], g is the standard acceleration of (Earth's) gravity, and P is the input power to the power processing unit(s) (PPUs):

$$T = 2\eta P/gI_{sp}, \qquad \dot{m} = 2\eta P/(gI_{sp})^2 \tag{6}$$

A specific impulse range of 1000–6000 s is used to survey the design space. However, actual thrusters can only throttle over a limited range, so the missions are also examined with an I_{sp} of 1600–2400 s (for Hall thrusters [11]) or 3600–4400 s (for ion thrusters).

While a single super engine provides a convenient model for mapping the design space, the actual propulsion system comprises multiple thrusters. It is often assumed that the power level P_0 drives the number of required thrusters. However, for missions to destinations beyond Earth's orbit, most of the actual thrusting is done at a much lower power level than P_0 (due to the inverse square of solar flux with heliocentric range). Instead, the propellant throughput m_p is a much better indicator to the number of required thrusters. As the engines process propellant, they degrade, and additional thrusters must be available to replace the old ones. This effect suggests that the mass and cost factors for propellant and thrusters may be combined. Table 1 provides a breakdown of the estimated mass and cost associated with the thrusters and propellant. It is stressed that these mass and cost values do not reflect the actual mass or cost of the system but, instead, account for variations within the system (i.e., relative comparisons).

E. Power and Processing Units

The solar array model is a simple inverse square curve, and it does not account for any thermal efficiencies or radiation inefficiencies. In Eq. (7), P is the power out of the solar arrays, P_0 is the array power at 1 astronomical unit (AU), and r is the radial distance from the sun:

$$P = P_0/r^2 \tag{7}$$

Spacecraft power is ignored and, for the purposes of this sizing exercise, only SEP power into the PPUs is included in Eq. (6). The primary reason spacecraft power is omitted is to ease the scaling of the power system with launch vehicle and spacecraft mass [as in Eq. (2)]. If the spacecraft is powered by the arrays (as opposed to a radioisotope thermoelectric generator), then P_0 typically increases by one to a few kilowatts, depending on how far from the sun the spacecraft operates. As with the launch vehicle model, it is informative to examine the design space with free choice of P_0; however, solar arrays are not typically built to any desired power level (arrays could be sized to the nearest 1 or 2 kW). Moreover, it is often economical to incorporate a standard array, say, from a previous mission or one being developed for another spacecraft. The solar array size is therefore limited to power levels of 5, 10, 15, 20, and 25 kW to examine the implications of nonoptimal P_0.

While the propellant throughput can provide a rough estimate of the number of thrusters, the optimal power level P_0 provides an estimate of the number of PPUs. It is usually not necessary to have enough PPUs to process all of the available power at 1 AU, but designs that converge to higher power levels typically require additional PPUs to operate additional thrusters. Moreover, a single PPU can cross strap to multiple (or at least a couple) thrusters, partially decoupling the number of PPUs to the number of thrusters. In this sense, the PPU cost and mass factors may be book kept with the power factors, as provided in Table 2. The key here is not to determine the absolute number of PPUs to be used (which can be chosen in subsequent design iterations) but, rather, to keep track of the relative mass and cost of the system for different designs (e.g., a 15 kW array is likely to use more PPUs than a 5 kW array).

Table 1 Mass and cost factors for thrusters and propellant

Component	Mass	Cost	Notes
Tankage	100 kg/t of m_p	\$1 million/t of m_p	Includes support structure.
Propellant	——	\$1 million/t of m_p	Cost of xenon.
Throughput	300 kg of m_p	——	Typical 5 kW thruster. Higher power limit or Hall may process more xenon.
Thruster	30 kg or 100 kg/t of throughput	\$3 million or \$10 million/t of throughput	Typical 5 kW thruster. Higher power limit involves additional mass and cost. Includes gimbal and feed system.
Total	$\mu_p = 200$ kg/t	$\chi_p =$ \$12 million/t	——

Table 2 Mass and cost factors for solar array and PPU

Component	Mass	Cost	Notes
Solar Array	10 kg/kW	\$1 million/kW	Relative values: do not include fixed mass or cost.
PPU	30 kg or 6 kg/kW for 5 kW thruster	\$3 million or \$0.6 million/kW for 5 kW thruster	Typical for 5 kW thrusters. Higher power limit involves additional mass and cost. Includes other power conditioning elements.
Total	$\mu_{P0} = 16$ kg/kW	$\$\chi_{P0} = 1.6$ million/kW	——

Table 3 Mass and cost parameters used to select SEP systems

Component	Mass	Cost	Notes
Operations	——	$\chi_{\text{TOF}} = \$10$ million/yr.	——
Launch vehicle	——	$\chi_{m0} = \$20$ million/t	Discrete levels are $m_0 = 1.5, 3.5, 5, 6.5$, or 9 t
Propellant	$\mu_p = 200$ kg/t	$\chi_p = \$12$ million/t	I_{sp} also limited to 1600–2400 or 3600–4400 s
Power	$\mu_{P0} = 16$ kg/kW	$\chi_{P0} = \$1.6$ million/kW	Discrete levels are $P_0 = 5, 10, 15, 20$, or 25 kW

F. Compilation of Modeling Parameters

The coefficients used to track changes in net mass and mission cost are summarized in Table 3. There are constant mass and cost values associated with these coefficients that are essentially added to the net mass values. For example, the solar array mass may follow 100 kg + 10 kg/kW (so a 10 kW array would have a specific mass of 20 kg/kW). The 100 kg is simply added to the desired net mass (which includes non-SEP components such as the payload and bus) and the 10 kg/kW is used to track mass variations due to P_0 among different designs, as in Eq. (1). Furthermore, if the array cost follows \$5 million + \$1 million/kW the \$5 million is tacked onto the fixed net mass cost (e.g., cost for scientific instruments) and the \$1 million/kW is used to optimize the design to a minimum cost solution using Eq. (5). The parameters in Table 3 are rough estimates based on past missions, the current market, and projected developments. These values are not meant to reflect actual values used for mission design but, rather, serve to illustrate a method of minimizing cost for a SEP mission.

III. Mission Descriptions

Optimal SEP systems can vary significantly for different missions; therefore, it is prudent to include a range of destinations and spacecraft masses when addressing the general problem of designing SEP missions. Although the mission set presented here is certainly not comprehensive (a target within Earth's orbit is a notable omission), it does include a variety of mission characteristics including (among others) relatively close and more distant destinations, rendezvous and sample returns, short and long flight times, small and large ΔV, and compact and massive spacecraft. The trajectories in Figs. 3–8 illustrate the general characteristics for each mission, but they do not reflect any actual design (i.e., the launch vehicle, flight time, power, and specific impulse are arbitrary). These trajectories are used as the initial guesses to MALTO, and the optimized missions would vary for different initial guesses (e.g., different launch year or number of heliocentric revolutions). Indeed, the theme is a process to modify suboptimal, potentially infeasible designs (e.g., Figs. 3–8) into cost-effective robust missions. In Figs. 3–8, the spacecraft path is the solid line, encounter body orbits are dotted lines, thrusting is noted by arrows, and encounters (launch, flyby, etc.) are circles.

A. Example Near-Earth Asteroid Sample Return

The assumed destination for this mission is the asteroid 1989 ML, which is the closest target to Earth in the set. Near-Earth asteroid missions typically involve lower power levels, because the spacecraft

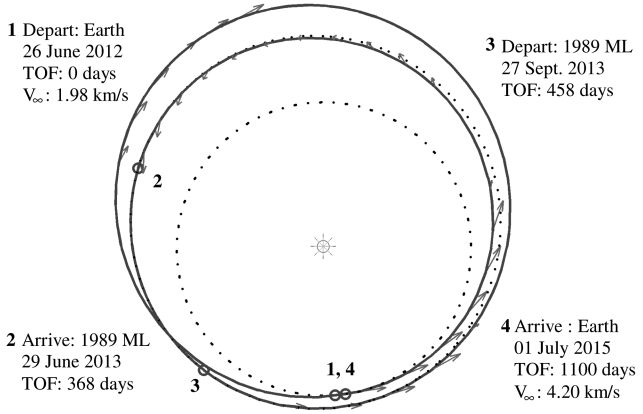

Fig. 3 Encounter bodies and times with spacecraft trajectory for an example asteroid sample return mission.

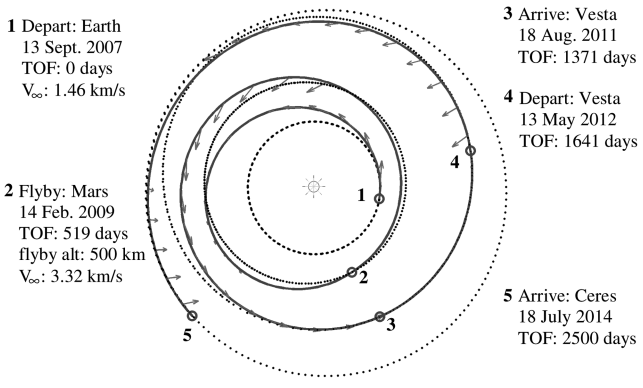

Fig. 4 Encounter bodies and times with spacecraft trajectory for example asteroid rendezvous mission.

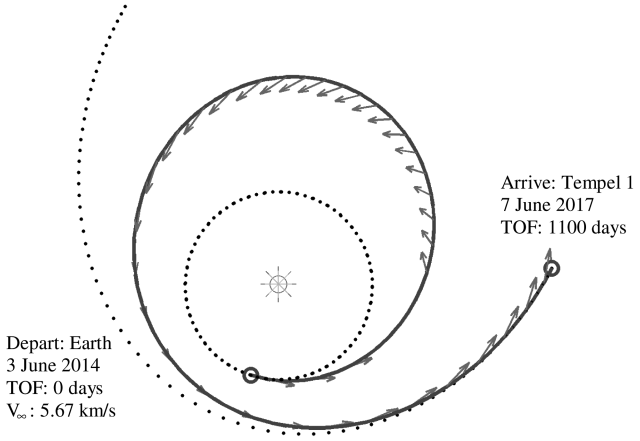

Fig. 5 Encounter bodies and times with spacecraft trajectory for comet rendezvous mission example.

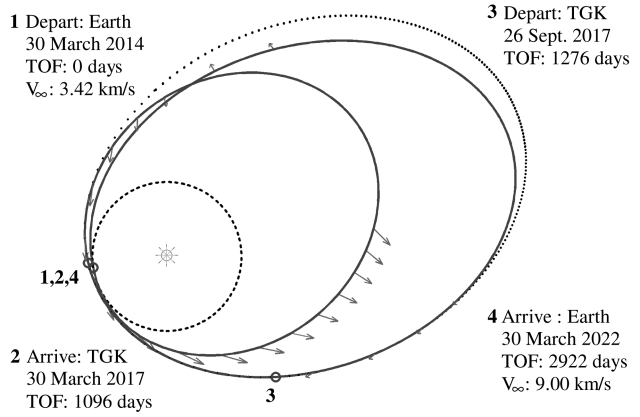

Fig. 6 Encounter bodies and times with spacecraft trajectory for comet sample return mission example.

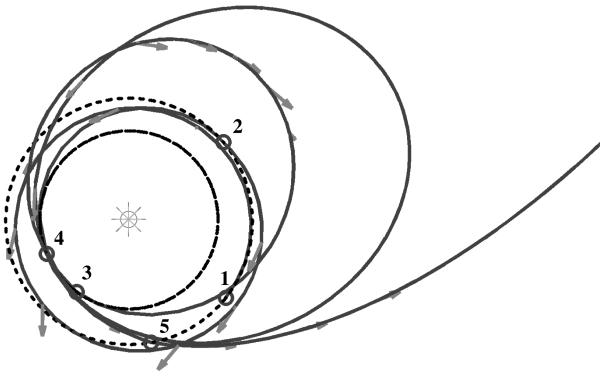

1 Depart: Earth	**2** Flyby: Earth	**3** Flyby: Venus	**4** Flyby: Venus	**5** Flyby: Earth
18 Aug. 2020	21 Nov. 2021	28 March 2022	31 May 2023	2 July 2025
TOF: 0 days	TOF: 519 days	TOF: 591 days	TOF: 1021 days	TOF: 1783 days
V_∞: 0.80 km/s	Flyby alt:15020 km	Flyby alt:710 km	Flyby alt:1080 km	Flyby alt:300 km
	V_∞: 3.32 km/s	V_∞: 6.00 km/s	V_∞: 8.48 km/s	V_∞: 16.0 km/s

Fig. 7 Flyby sequence and zoom on inner planet portion of trajectory for example mission to Saturn.

is never too far from the sun. The assumed net mass for this mission is 1600 kg, which is larger than a rendezvous spacecraft but smaller than an outer planet mission. Thus, there is an interesting combination of low ΔV with moderate mass. The assumed mission duration is around three years, with a minimum 90-day stay time.

B. Example Main Belt Asteroid Rendezvous

The body sequence for this example mission includes a Mars flyby, Vesta rendezvous and departure, and Ceres rendezvous (same path as Dawn). Because it is a rendezvous mission, the assumed net mass is 800 kg (no need for return hardware as with a sample return), but the ΔV is large (10–14 km/s) because there are two rendezvous assumed. So, this mission is an example of a small spacecraft combined with a large ΔV. It also provides an example with multiple destinations. Missions to the main belt often allow a wide range of flight times (with different heliocentric revolutions), so a TOF range of 4–10 years is examined. The minimum stay time at Vesta is assumed to be 270 days.

C. Comet Rendezvous Example

The assumed rendezvous target is Tempel 1, which is a Jupiter-family comet (aphelion is near Jupiter's orbit). The net mass is the same as the asteroid rendezvous example, 800 kg. This mission provides an example of a small spacecraft with a moderate ΔV target. Rendezvous usually occurs within a year after perihelion, and the range at rendezvous is between 1.5–3 AU. This example is also notable because the spacecraft thrusts almost the entire way to the comet.

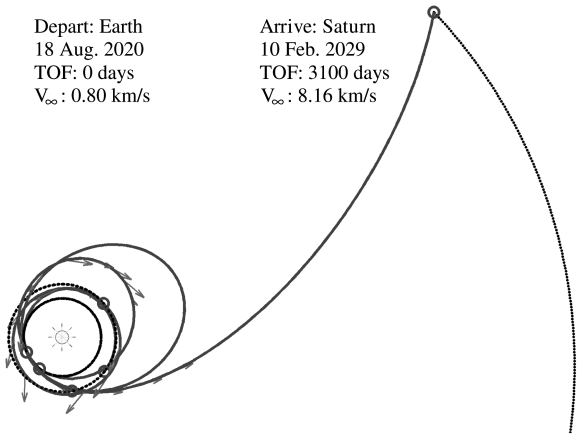

Fig. 8 Spacecraft trajectory for example mission to Saturn.

D. Comet Sample Return Example

The target for this example is another Jupiter-family comet, Tuttle–Giacobini–Kresak (TGK). This mission combines a moderate-sized spacecraft (net mass for sample returns assumed to be 1600 kg) with a large ΔV. Comet sample returns stress a SEP system, because the spacecraft must often thrust at far distances from the sun (up to 4 AU) to depart the comet. As a result, these missions typically involve the largest solar arrays. Also, entry speeds at Earth can become prohibitively high, so the arrival V_∞ is limited to 9 km/s. This constraint is almost always active. The assumed mission duration is around eight years, with a minimum 180-day stay at the comet.

E. Outer Planet Example

The final example in the set is a mission to an outer planet: Saturn. Because of Saturn's great distance from the sun (9–10 AU), a SEP stage is impractical for orbit insertion. Instead, the means of rendezvous at Saturn is not specified (e.g., chemical stage or aerocapture), but the arrival V_∞ is limited to 9 km/s. This constraint becomes active at shorter flight times. Most of the ΔV to reach Saturn is achieved by gravity assists, making this example unique in the set. (The body sequence is Earth–Earth–Venus–Venus–Earth–Saturn.) Moreover, while the destination is distant, most of the thrusting occurs near Earth's orbit (0.7–2 AU), so this mission also provides an example where most of the ΔV is imparted near the sun. A net mass of 4500 kg is chosen to reflect a flagship class mission, providing an example of a massive spacecraft with small propulsive ΔV and large gravity assist ΔV.

F. Overview of Example Mission Set

A set of pertinent characteristics of the example missions are combined in Table 4. The net masses do not reflect any actual spacecraft but, instead, serve to offer a variety of SEP system designs.

IV. Solar Electric Propulsion System Selection

When a mission is first proposed, the design space is remarkably open. The study typically begins with a target of scientific interest and method of investigating the target. Major design choices such as launch vehicle, solar array power, number of thrusters, and engine type remain to be determined. (The propellant load is also a design variable, but it is largely a function of the selected specific impulse.) The required net (non-SEP dependent) mass of the spacecraft usually converges quickly based on the instrument package, and a cursory trajectory search can determine if the desired target is attainable in the time frame of interest. From this initial search (e.g., beginning with the trajectories in Figs. 3–8), the design team must find a robust system configuration that can reliably deliver the net mass to the

Table 4 Summary of example mission parameters

Example mission	Assumed destination	Net mass, kg	TOF, yr	ΔV, km/s	Thrust distance, AU	Spacecraft distance, AU
Asteroid sample return	1989 ML	1600	~3.	~3	1–1.6	1–1.6
Asteroid rendezvous	Vesta and Ceres	800	4–10	10–14	1–2.5	1–3
Comet rendezvous	Tempel 1	800	2.5–6	~8	1–3	1–4
Comet sample return	TGK	1600	~8.	12–16	1–4	1–5
Outer planet	Saturn	4500	7.5–11	2–5	0.7–2	0.7–10

target, and that is unlikely to require dramatic changes when the spacecraft mass fluctuates. This problem is twofold: first, how does one arrive at a robust design; then, how does one determine if the selected system is better than all of the other robust designs? Because of the multifaceted nature of SEP missions, there are myriad solutions that provide the same mass margin (the allocated performance above the estimated requirement is a key factor for mission robustness), and established methods that point the way to robust chemical systems (e.g., minimize ΔV) are insufficient to distinguish one SEP design from another. For example, maximizing the delivered mass fraction is useful for selecting a launch vehicle and thruster specific impulse but provides little guidance to size the power and propulsion system. Net mass optimization accounts for the power and propulsion system but leaves the flight time as a free parameter. The proposed approach is to depart from mass optimizations and use dollar cost to unite the selection of launch vehicle, power and propulsion system, and flight time into a single figure of merit.

While this cost approach arrives at designs that balance the launch vehicle, SEP system, and flight time, it does not necessarily ensure robustness. For example, the cost optimization may arrive at a design point that is very near the maximum net mass fraction so that the spacecraft can fit on a small (and inexpensive) launch vehicle. But, if the payload or hardware mass increases, the launch mass may exceed the capability of the launch vehicle, and a new design is required. One way to track the system sensitivity to spacecraft mass is to create a set of minimum cost solutions over a range of net masses. The increased margin on net mass also absorbs increases in hardware mass. If a system is designed for a net mass of 1000 kg, but the current net mass estimate is 900 kg, then a 100 kg increase in payload or a 100 kg increase in propulsion system mass are absorbed equally into the 1000 kg allocation. In this way, the minimum cost solution for any desired mass margin is determined.

The SEP system selection process centers on the minimum cost performance and associated designs, shown in Figs. 9–18, where the net mass is varied by ±30% for each mission. The TOF for mass optimizations is constrained to the cost-optimal value to provide consistent missions. The bold curve (also denoted by the ◯ symbol) in these figures corresponds to the minimum cost solution with discrete choice of launch vehicle, array size, and specific impulse (at the levels specified in Table 3). These results are compared with the continuous parameter set (e.g., free choice of launch vehicle size) and with solutions obtained by maximizing net mass fraction m_N/m_0 and delivered mass fraction m_f/m_0. The discrete m_N/m_0 curves are denoted by a ∇, while the discrete m_f/m_0 optimizations are denoted by a Δ, so when they happen to be equal, they appear as a hexagram. The continuous m_N/m_0 and m_f/m_0 optimizations are omitted in Figs. 9–18 for clarity.

A. Near-Earth Asteroid Sample Return Example

As indicated by the flat bold curve in Fig. 9, a variation in net mass allocation does not strongly affect the cost of this example mission. From Fig. 10, the launch vehicle, power system, and flight time are constant (bold curves) near the target net mass of 1600 kg. (The launch vehicle and P_0 values in Fig. 10 are rounded up to the discrete values of 3.5 t and 5 kW, as specified in Table 3, to calculate cost.) The specific impulse curve indicates how the system allocates more mass. The I_{sp} steadily drops from 4400 s at 1600 kg to 3600 s at 2000 kg, so it appears that the cost-optimal mechanism to increase net mass is to burn more propellant to complete the mission. As noted in Table 4, the ΔV for this example is quite low, so changes in the design should have little impact on propellant mass. The impact on cost appears in the very slight slope of the bold cost curve in Fig. 9. Thus, the SEP system could be designed to a net mass of 2000 kg, providing plenty of margin with little impact on cost.

If a net mass optimization method were used instead of cost optimization, the resulting system configuration would cost about $10 million more (∇ curve in Fig. 9). The difference in cost arises from the mass-optimal configuration converging to a solution with more power. The high power solutions found via mass optimization are essentially used to build the launch vehicle margin into the system as opposed to reducing cost. The launch vehicle subplot in Fig. 10 shows that the spacecraft only uses a fraction of the launch vehicle capability (of 3.5 t at escape). While this discrepancy between launch vehicle requirement and capability builds margin into the system, it is not a cost-effective design. Instead, if a 25% mass margin is desired, then the cost-optimal design with 2000 kg net mass should be sought.

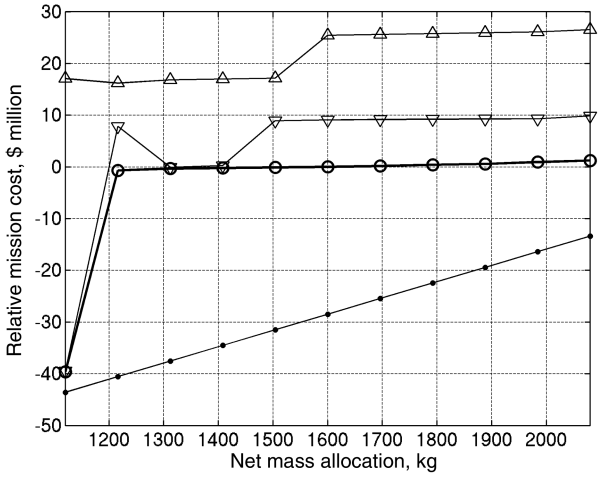

Fig. 9 Mission cost for asteroid sample return example, where ◯ = cost, ∇ = m_N/m_0, Δ = m_f/m_0 optimizations for discrete system levels (Table 3), and ● = cost solutions with continuous systems.

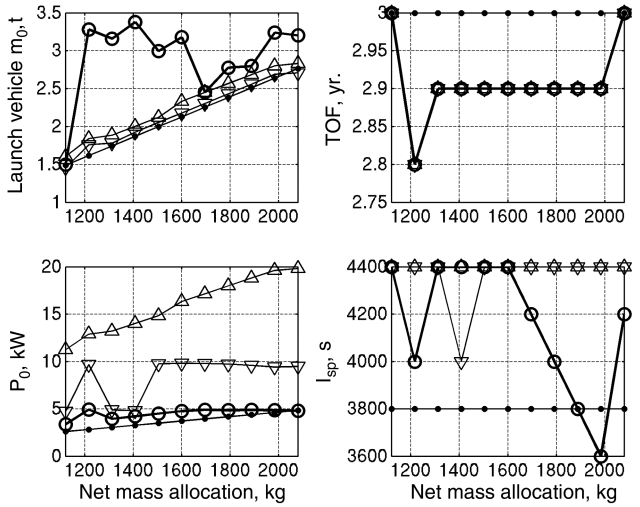

Fig. 10 SEP system designs corresponding to Fig. 9.

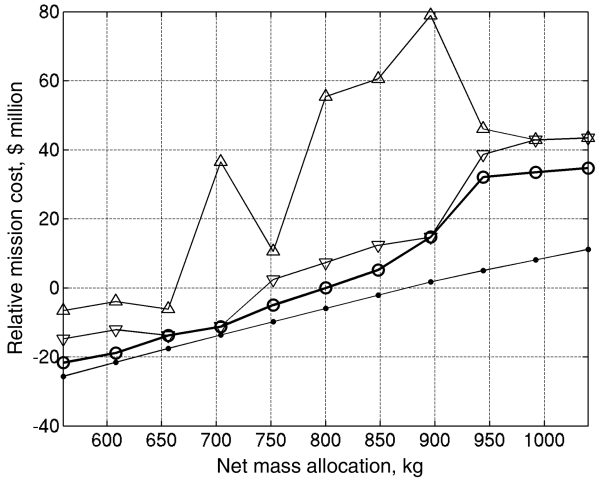

Fig. 11 Mission cost for asteroid rendezvous example, where ◯ = cost, ∇ = m_N/m_0, Δ = m_f/m_0 optimizations for discrete system levels (Table 3), and ● = cost solutions with continuous systems.

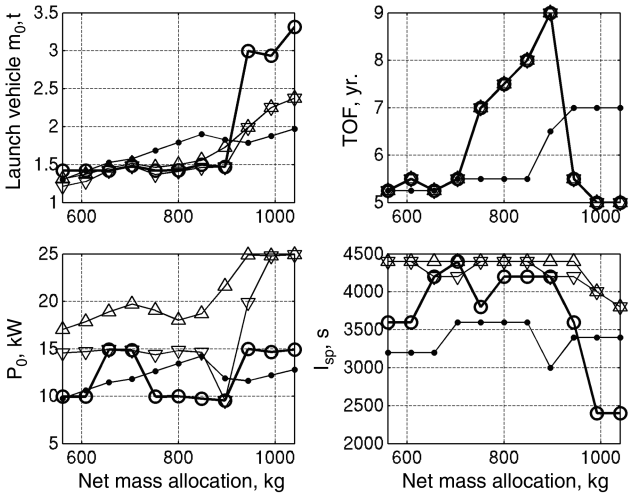

Fig. 12 SEP system designs corresponding to Fig. 11.

While the chosen search method has a significant effect on which combination of systems is deemed optimal, the limited set of hardware options can have an even larger effect on mission cost. As indicated by the continuous system curve (denoted by ●) in Fig. 9, the mission could save about $30 million if the optimal configuration were available. (The ● point is $30 million lower than the ◯ point at the nominal mass of 1600 kg.) From Fig. 10, the optimal launch vehicle size has a m_0 of around 2 t and, at $20 million/t, would cost about $30 million less than the available 3.5 t vehicle. But when only large launch vehicles are available, the cost-optimization method automatically finds solutions that make use of the excess launch vehicle capability by keeping the power system small and slightly reducing flight time. We note that, for a fixed net mass, it is usually not advantageous to use the full launch vehicle capability; hence, the cost-optimal m_0 in Fig. 10 does not optimize to the full 3.5 t discrete value (even though the full value is reflected in the cost). The key mechanism for this behavior is cost dependence on propellant mass. If the system were designed with a higher launch mass, then more propellant would need to be expended to reach the fixed net mass, and the overall cost would be higher. By lowering the launch mass below the full launch vehicle capability, the spacecraft can fly a more efficient trajectory due to the higher acceleration for a given thrust, and less propellant and cost are required to accomplish the mission.

B. Main Belt Asteroid Rendezvous Example

This example mission exhibits a stronger correlation between net mass and mission cost than the asteroid sample return example. The mission cost increases consistently up to about 900 kg net mass (800 kg is the design requirement). From Fig. 12, the $15 million jump in cost in the bold discrete system curve occurs because the launch vehicle switches from the 1.5 to the 3.5 t model. Up to this point, the increase in net mass is handled by increasing flight time. Then, when the mass becomes large enough, the cost-optimal configuration switches from a small launch vehicle with a long flight time to a large launch vehicle with short flight time. The $40 million price tag for switching to the larger launch vehicle is largely offset by the dramatic reduction in flight time. Also, the power system increases, and the thruster I_{sp} decreases to provide more thrust to accelerate the larger vehicle on the short TOF trajectory. Between 900 and 1000 kg, both designs (small vehicle with long flight time vs large vehicle with short flight time) are available, but the solution found by optimizing cost is to switch to short flight times with a larger launch capability. A similar trade occurs on the lower end of the net mass scale. Between 600 and 700 kg, an increase in power to 15 kW handles the mass increase, then from 700 to 800 kg, the flight time is increased and the power drops back down to 10 kW. In this way, cost optimization aids the decision on when it is more beneficial to increase power, flight time, or launch vehicle to build margin into the system. Since the SEP system configuration at the nominal 800 kg can absorb at least a 100 kg increase in net mass without redesigning the hardware, the 800 kg configuration is selected for this mission. This SEP system demonstrates robustness by handling mass growth with flight-time margin.

The continuous system solution also increases flight time to absorb mass increases but, in this case, the impact on cost is not as dramatic because the launch vehicle and power system adjust smoothly to balance against the change in TOF. The cost-optimal SEP solution is to increase launch vehicle and power until the net mass reaches about 850 kg, then the launch and power systems return to a smaller size once the flight time begins to rise. Thus, the optimal cost curve (● line) in Fig. 11 remains nearly linear across this boundary.

The optimal delivered mass solution has a significantly higher cost than the other solutions across the net mass range. From Fig. 12, it is apparent that a primary cause for the additional cost is high power levels. For a given launch vehicle, the largest delivered mass is attained by increasing power. The concept of net mass optimization was introduced to account for the mass of the power and propulsion system while maximizing payload allocation. In this way, the SEP system can be optimized to allocate more net mass, as indicated by the lower power levels (∇ vs Δ) in Fig. 12. However, optimizing the net mass fraction leads to the smallest launch vehicle for a given net mass, which can lead to superfluous mass margins. Instead, this extra margin could be paid back in reduced mission cost. So, just as

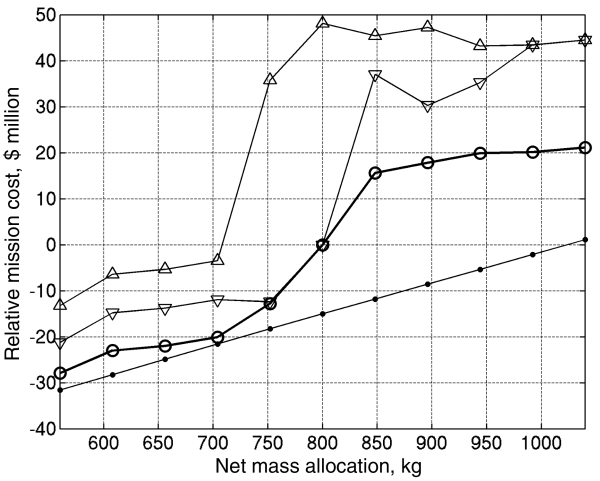

Fig. 13 Mission cost for comet rendezvous example, where ◯ = cost, ∇ = m_N/m_0, Δ = m_f/m_0 optimizations for discrete system levels (Table 3), and ● = cost solutions with continuous systems.

delivered mass optimizations can lead to an underutilization of spacecraft ability to maximize payload [10], net mass optimizations can lead to an underutilization of launch vehicle ability to reduce mission cost.

C. Comet Rendezvous Example

This example mission presents an interesting case where the cost-optimal system has a dramatic shift almost right at the nominal net mass design point. In Fig. 13, the bold optimal cost curve is relatively flat for net masses that are much more or much less than the nominal value. Figure 14 shows the design in transition at 800 kg net mass. Beginning at 550 kg, the system tends to continue increasing power to account for the increasing net mass. Then, around 800 kg, the flight time must increase dramatically to accommodate the large net mass on the small launch vehicle. For larger spacecraft, it is cost effective to reduce the flight time to around 2.5 years with more thrust (lower I_{sp}) on a larger launch vehicle. The mass fraction is dramatically decreased at this transition as the trajectory switches from low ΔV with high I_{sp} to large ΔV with low I_{sp}, thus making full use of the launch vehicle capability. Since the net mass tends to increase as the design matures, the selected SEP system should correspond to the cost-optimal solution for larger net masses. This case has the unique property of requiring a lot of cost for a little mass margin (e.g., going from 800 to 850 kg), but then large increases in mass (e.g., going from 850 to 1050 kg) may be accommodated with relatively little cost.

The cost-optimal design points with more than 900 kg net mass allocation are significantly different than the mass-optimal designs that provide the same mass margin in Fig. 14. Specifically, the launch vehicle is much larger, and the power and specific impulse are lower than the other solutions. Indeed, the cost-optimal designs are usually distinct from the mass-optimal solutions, which are comparatively similar to each other. This behavior is most evident in the optimal launch vehicle m_0 curves. A basic purpose to optimize net mass is to find solutions that are fundamentally different than optimal delivered mass designs. However, for the mass parameters in Table 3, the two solutions are usually similar, as the power and propulsion mass coefficients do not sufficiently differentiate the designs. A distinguishing characteristic of the cost approach is that there are more parameters that affect the optimization, which leads to distinct SEP system designs. In this way, the optimal solution space (i.e., the locus of designs found by the optimizer) is broadened, reducing the number of trade studies required to arrive at cost-effective solutions.

D. Comet Sample Return Example

The cost-optimal design for this example mission requires a dramatic shift in system parameters for any mass growth above the nominal 1600 kg net mass allocation. Just as with the comet rendezvous example, an increase in net mass is most easily accommodated by switching to a larger launch vehicle. But unlike the comet rendezvous example, the shift in cost for the discrete parameter set (bold line in Fig. 15) does not level off after the launch vehicle change. Instead, the mission cost rises proportionally with the net mass over a wide mass range. The cost-optimal design choices that allocate increasing net mass may be inferred from Fig. 16. First, a nine-month jump in TOF provides room to fit the 1600 kg nominal mass on the 3.5 t launch vehicle. Then, the design shifts to a bigger launch vehicle at 1700 kg; the power rises at 1800 kg; the propellant load increases (I_{sp} decreases) at 1900 kg; then, the cycle is repeated by increasing TOF again at 2000 kg net mass. So, for this mission, there is no single mechanism that consistently allocates larger mass, which helps explain why the cost does not level off at the launch vehicle switch. Since it appears that every 100 kg increase in net mass corresponds to a \$10 million increase in cost, the selected SEP system is a strong function of the desired mass margin. In this case, a 100 kg margin is assumed, placing the system on a larger launch vehicle with 20 kW of power and high specific impulse for the SEP system. The optimal TOF for this system is 8.0 years, which places the design right in the middle of the flight-time range (noted in Table 4), so lowering TOF could help reduce cost at the nominal 1600 kg point, while there is room to increase the TOF to accommodate masses beyond 1700 kg. In this case, changing the flight time is not the cost-optimal choice (at least before hardware is designed and built), but it provides a mechanism to adjust the mass margin without affecting the spacecraft design.

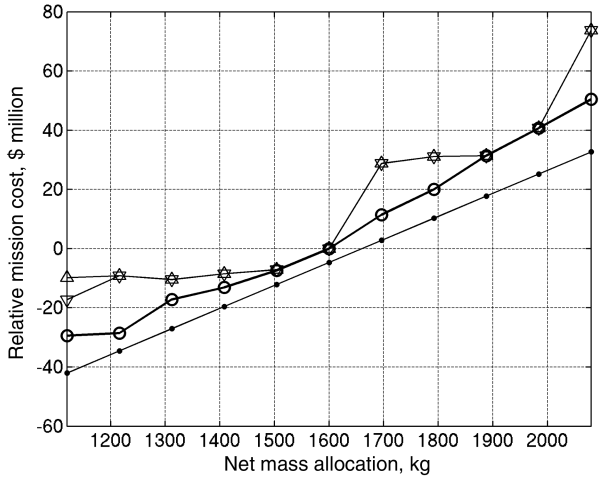

Fig. 15 Mission cost for comet sample return example, where ○ = cost, ∇ = m_N/m_0, Δ = m_f/m_0 optimizations for discrete system levels (Table 3), and ● = cost solutions with continuous systems.

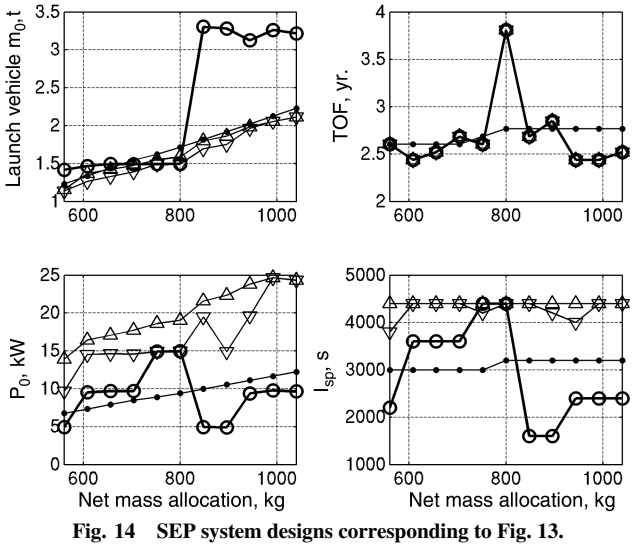

Fig. 14 SEP system designs corresponding to Fig. 13.

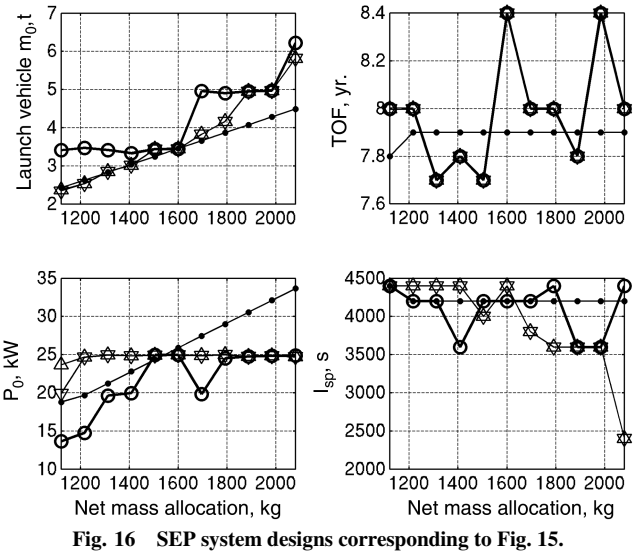

Fig. 16 SEP system designs corresponding to Fig. 15.

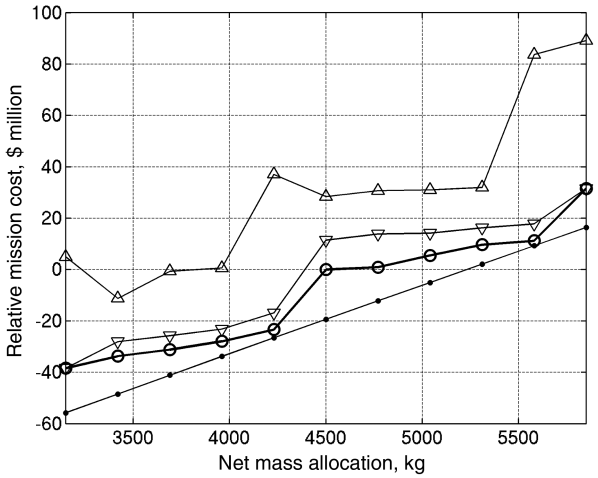

Fig. 17 Mission cost for example mission to Saturn, where ○ = cost, ∇ = m_N/m_0, Δ = m_f/m_0 optimizations for discrete system levels (Table 3), and ● = cost solutions with continuous systems.

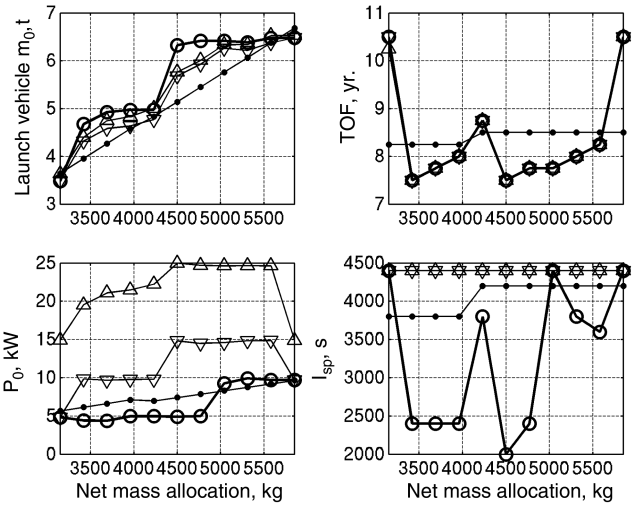

Fig. 18 SEP system designs corresponding to Fig. 17.

This example mission is unique in that the optimal discrete system solution lines up with the optimal continuous parameter solution at the nominal point. From the ● curves in Fig. 16, the cost-optimal m_0 is around 3.5 t, the optimal P_0 is just above 25 kW, and the optimal I_{sp} is at 4200 s. The discrete system flight time is longer than the continuous solution to absorb the small variations from the optimal. Indeed, over the entire examined net mass range, the discrete system cost is relatively close to the continuous model cost. The two solutions begin to diverge slightly after 1800 kg as the maximum allowable P_0 of 25 kW constrains the system. (A 30 kW array would lower mission cost at high masses.)

Because the discrete and continuous solutions converge at the nominal, it is easy to begin with the optimal continuous solution (which usually requires less optimization work) and automatically see where the discrete solution should lie. However, the optimal continuous solution crosses the discrete level sets at only a few special points, so intermediate designs (between these points) are less straightforward. Even though the best direction to move when switching from a continuous model to a discrete model is not known a priori, the optimal discrete variables usually bound the optimal continuous solution. Thus, the continuous design answer (solvable with local optimization techniques) would make a good initial guess for a global optimization of the discrete solution space.

E. Outer Planet Example

The final example combines the trajectory efficiency of gravity assists with the propulsive efficiency of SEP. As with the comet mission examples, a cost-optimal switch in launch vehicle occurs near the nominal net mass, but this time, the switch occurs before the nominal value, so incorporating mass margin is not as costly. From the bold curve in the TOF plot in Fig. 18, the cost-optimal approach to increasing net mass before the launch vehicle switch at 4500 kg is to increase flight time. Then, a larger launch vehicle becomes more cost effective than increasing flight time, even though the launch vehicle costs $30 million more than the smaller model and additional TOF up to 10.5 years is available. From Fig. 17, the cost levels off for net masses above 4500 kg, and a 500 kg margin increases cost by only about $5 million, which provides some margin for mass growth. This design has a P_0 and I_{sp} that are near the continuous solution values, but the launch vehicle is larger than optimal (which is usually the case), and the flight time is lower than the continuous solution to partially offset the launch vehicle cost. At 5000 kg net mass, the cost difference between the discrete systems solution and the continuous solution is several million dollars, but at 5600 kg, where the optimal launch vehicle size for both continuous and discrete is 6.5 t, the mission costs are nearly identical.

Because of the low ΔV of this example mission (achieved via gravity assist), the mass fractions are naturally close to unity. (The asteroid sample return mission provides another low ΔV example.) Significant changes in P_0 and I_{sp} do not affect m_0 as much as missions with higher ΔV, because the SEP system does comparatively less work. However, significant changes in the SEP system still produce significant changes in cost. For this example, it appears that the cost-optimal design choice is to lower P_0 at the expense of additional propellant (with the lower I_{sp}). The optimal net mass solution has a slightly higher P_0, leading to slightly more mission cost, and achieves high mass fractions by increasing the I_{sp} to lower propellant mass. The optimal delivered mass solution lowers propellant mass even further with a much larger P_0, but it costs much more to fit the required net mass. In contrast with the other examples, the net mass optimization more closely corresponds to the cost-optimal solution, where the difference in cost is only $5–10 million for discrete system levels.

F. Chosen Mission Designs

The selected designs for the five example missions are compiled in Table 5. The designs correspond to a cost-optimal discrete value solution to minimize mission cost while providing net mass allocation above the nominal to ensure a robust design. At the inception of a mission concept, before the major design parameters are finalized, a healthy mass margin is usually warranted, but the appropriate amount is somewhat arbitrary. Once a SEP system is chosen and the

Table 5 Selected SEP systems, launch vehicles, and flight times

Example mission	Net mass, kg (margin)	m_0, t	TOF, yr.	P_0, kW	I_{sp}	Design cost $ million above 0% margin	Cost-optimal margin parameter
Asteroid sample return	2000 (400)	3.5	3	5	High	1	Propellant (I_{sp})
Asteroid rendezvous	900 (100)	1.5	9	10	High	15	Flight time
Comet rendezvous	1000 (200)	3.5	2.5	10	Low	20	Launch vehicle
Comet sample return	1700 (100)	5	8	20	High	10	All are effective
Outer planet	5000 (500)	6.5	7.75	10	High	5	Power and flight time

spacecraft construction begins, the individual system margins (e.g., power or propulsion) become a better indicator of the robustness of a mission [12]. Although the cost to modify any of these systems (i.e., the parameters in Table 3) changes throughout the mission, the process of explicitly solving for the cost-optimal design for the required payload still applies for any given design weights. The cost-optimization approach provides an efficient method of optimizing changes to the baseline mission (e.g., a change in payload or discontinuation of launch vehicle) when the desired mission margins and system costs fluctuate across mission phases.

V. Conclusions

Mission cost provides a figure of merit that combines the selection of launch vehicle, flight time, power system, and propulsion system into a single optimization problem. A single trade study of minimum mission cost over a range of net mass values then indicates the optimal system configuration for any desired mass margin. When more mass margin becomes necessary, the cost-optimal system parameter varies between mission types, obfuscating a priori decisions of the best SEP system for a mission. Sufficiently large increases in mass must be accommodated by increasing the launch vehicle capability, but the considerable increase in cost associated with a bigger launch vehicle is offset by decreasing flight time, power level, and/or propellant mass, where the optimization process determines the best balance of mission parameters. It is found that the cost-optimal configuration is generally not mass optimal, and mass-optimal designs are usually not cost optimal. Thus, mass fraction optimizations are usually insufficient to determine the minimum cost solution without brute force searches. Discrete levels in system parameters (e.g., gaps in launch vehicle size) can cause a dramatic increase in mission cost when compared with the optimal value for continuous systems. However, the optimal continuous system configuration supplies an initial approach to optimize the discrete system set, thus producing a cost-efficient design for the mission.

Acknowledgments

The work described in this publication was carried out at the Jet Propulsion Laboratory, California Institute of Technology, under a contract with NASA. The authors would like to acknowledge John Brophy, Bahrat Chudasama, Phil Garrison, Dan Goebel, Steve Larson, Earl Maize, and Stacy Weinstein for their support. The first author particularly thanks Theresa Kowalkowski and Jon Sims for their guidance on how to design missions with electric propulsion and also thanks Try Lam and Dan Lyons for their keen edits and insightful comments.

References

[1] Rayman, M. D., Fraschetti, T. C., Raymond, C. A., and Russell, C. T., "Coupling of System Resource Margins Through the Use of Electric Propulsion: Implications in Preparing for the Dawn Mission to Ceres and Vesta," *Acta Astronautica*, Vol. 60, Nos. 10–11, 2007, pp. 930–938. doi:10.1016/j.actaastro.2006.11.012

[2] Camino, O., Alonso, M., Gestal, D., de Bruin, J., Rathsman, P., Kugelberg, J., Bodin, P., Ricken, S., Blake, R., Voss, P. P., and Stagnaro, L., "SMART-1 Operations Experience and Lessons Learnt," *Acta Astronautica*, Vol. 61, Nos. 1–6, 2007, pp. 203–222. doi:10.1016/j.actaastro.2007.01.042

[3] Kawaguchi, J., Kuninaka, H., Fujiwara, A., and Uesugi, T., "MUSES-C: Its Launch and Early Orbit Operations," *Acta Astronautica*, Vol. 59, Nos. 8–11, 2006, pp. 669–678. doi:10.1016/j.actaastro.2005.07.002

[4] Zola, C. L., "A Method for Approximating Propellant Requirements of Low-Thrust Trajectories," NASA TN D-3400, 1966.

[5] Rayman, M. D., and Williams, S. N., "Design of the First Interplanetary Solar Electric Propulsion Mission," *Journal of Spacecraft and Rockets*, Vol. 39, No. 4, 2002, pp. 589–595. doi:10.2514/2.3848

[6] Auweter-Kurtz, M., and Kurtz, H., "Optimization of Electric Thrusters for Primary Propulsion Based on the Rocket Equation," *Journal of Propulsion and Power*, Vol. 19, No. 3, 2003, pp. 413–423. doi:10.2514/2.6124

[7] Sims, J. A., Finlayson, P. A., Rinderle, E. A., Vavrina, M. A., and Kowalkowski, T. D., "Implementation of a Low-Thrust Trajectory Optimization Algorithm for Preliminary Design," AIAA/AAS Astrodynamics Specialist Conference, Keystone, CO, AIAA Paper 2006-6746, Aug. 2006.

[8] Gill, P. E., "User's Guide for SNOPT Version 7: A FORTRAN Package for Large-Scale Nonlinear Programming," Univ. of California, San Diego, Dec. 2004.

[9] Landau, D. F., and Longuski, J. M., "Trajectories for Human Missions to Mars, Part II: Low-Thrust Transfers," *Journal of Spacecraft and Rockets*, Vol. 43, No. 5, 2006, pp. 1043–1048. doi:10.2514/1.21954

[10] Patel, P., Scheeres, D., and Gallimore, A., "Maximizing Payload Mass Fractions of Spacecraft for Interplanetary Electric Propulsion Missions," *Journal of Spacecraft and Rockets*, Vol. 43, No. 4, 2006, pp. 822–827. doi:10.2514/1.17433

[11] Hofer, R. R., "High-Specific Impulse Operation of the BPT-4000 Hall Thruster for NASA Science Missions," AIAA Paper 2010-6623, July 2010.

[12] Oh, D. Y., Landau, D., Randolph, T., Timmerman, P., Chase, J., Sims, J., and Kowalkowski, T., "Analysis of System Margins on Deep Space Missions Utilizing Solar Electric Propulsion," AIAA/ASME/SAE/ASEE Joint Propulsion Conference, Hartford, CT, AIAA Paper 2008-5286, July 2008.

J. Martin
Associate Editor